American Journal of Mechanical Engineering, 2014, Vol. 2, No. 7, 219-225
Available online at http://pubs.sciepub.com/ajme/2/7/10

DOI:10.12691/ajme-2-7-10

Design of Mobile Inspection Robot

Ivan Virgala[1,*], Michal Kelemen[1], Tatiana Kelemenová[2], Tomáš Lipták[1], Matej Poláček[1]

[1]Department of Mechatronics, Technical University of Košice / Faculty of Mechanical Engineering, Košice, Slovakia
[2]Department of Biomedical Engineering and Measurement, Technical University of Košice / Faculty of Mechanical Engineering, Košice, Slovakia
*Corresponding author: ivan.virgala@tuke.sk

Received September 08, 2014; Revised September 29, 2014; Accepted October 15, 2014

Abstract The aim of the paper is to design of mechanical and electronic parts of mobile inspection robot, which is designed for car undercarriage inspection tasks purposes. At first, mathematical model of robot motion on inclined plane is introduced, by which the actuators can be designed. Subsequently, driving and powered axle are designed with their particular parts. In the next section, design of particular electronic parts is introduced. In the conclusion the final version robot is shown.

Keywords: *electronics, inspection, mechanics, robot*

Cite This Article: Ivan Virgala, Michal Kelemen, Tatiana Kelemenová, Tomáš Lipták, and Matej Poláček, "Design of Mobile Inspection Robot." *American Journal of Mechanical Engineering*, vol. 2, no. 7 (2014): 219-225. doi: 10.12691/ajme-2-7-10.

1. Introduction

Nowadays, at the time of increasing terrorist attacks, the safety is often used word. Human life is endangered during ordinary day especially in troubled countries. A man is irreplaceable and therefore robots are used in the areas where it is dangerous.

The paper presents design of tank chassis robot for inspection of car undercarriage purposes. The robot is able to move under car and by means of two cameras is able to monitor the undercarriage. The robot is controlled by user using radio control.

Concept of the robot is simple but effective for inspection tasks. In the following sections will be dealt with mechanical design and design of particular electronic components.

2. Design of Mechanical Parts of Robot

Mechanical design is based on simple concept of robot which is reliable and effective. The aim of the robot is inspection of car undercarriage, because of presence of explosives. Therefore the height of the robot has to be lower than ride height. The basic concept of the robot in the Figure 1 is shown.

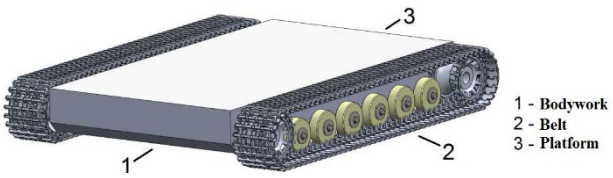

Figure 1. Basic concept of designed inspection robot

2.1. Design of Bodywork and Platform

After choosing suitable concept of the robot, the next step is design of basic dimensions and shape of bodywork and platform with choice of suitable material. The shape and dimensions were designed so, that robot would be simple and robust.

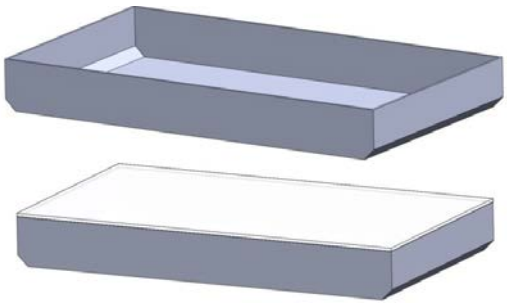

Figure 2. Bodywork with platform of robot

In this phase, dimensions of robot are only approximate. Accurate dimensions will be defined after designing all necessary components. Particular dimensions of main parts are in the following figure.

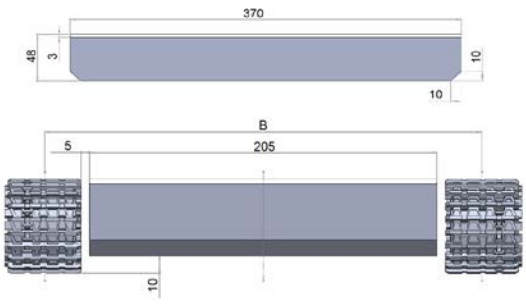

Figure 3. Preliminary dimensions of bodywork with platform

Chosen material of bodywork is aluminium alloy EN AW-3103.

2.2. Design of Robot Actuators

Assuming mentioned dimensions and shape of bodywork, the actuators can be designed. Designing of the actuators is one of the important points during whole process. Choice of suitable actuator for robot motion is determined by considering and describing forces, which act on robot during its motion.

There are several resistance forces acting on the moving on tank chassis robot. Direction and orientation of these forces in the Figure 4 are drawn. For simplification, there is consideration, that tank chassis behaves like rigid beam.

2.2.1. Linear Motion of Robot on Inclined Plane

Forces, acting on the moving tank chassis robot in the Figure 4 are drawn.

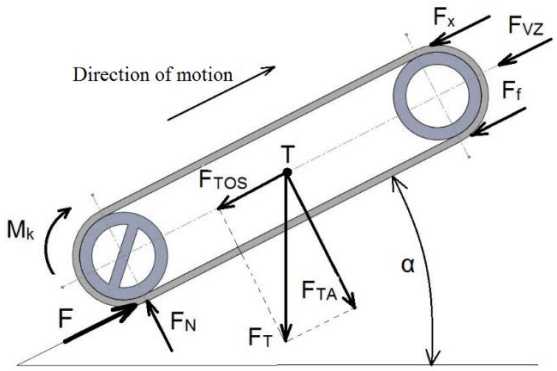

Figure 4. Forces affecting moving robot on slip plane

where F is propulsive force, M_k is torque on driving wheel, α is angle of plane slope, T is central of gravity, F_{VZ} is aerodynamic resistance, F_x is force of inertia, F_T is gravity, F_{TA} is component of gravity which is perpendicular to surface, F_{TOS} is component of gravity parallel with surface, F_N is normal force and F_f is rolling-resistance force. Based on the Figure 4, it can be written following system of equations.

$$F_{OUT} = F_{VZ} + F_x + F_f + F_{TOS} \tag{1}$$

$$F > F_{OUT} \tag{2}$$

$$M_K = \frac{Fr_H}{2} \tag{3}$$

$$F_{VZ} = \frac{\rho c_x P v^2}{2} \tag{4}$$

$$F_f = fF_N \tag{5}$$

where f is coefficient of rolling-resistance force which depends on type of surface. For calculation is used value 0,25 which presents snow surface. Coefficient ρ is specific weight of air, ρ = 1,4 kgm^{-3}. Coefficient of aerodynamic resistance c_x is 1,05. Constant P presents facing place.

$$\eta_T = \eta_{PA}\eta_{PR}\eta_{PM} \tag{6}$$

where η_{PA}, η_{PR} and η_{PM} represent coefficient of effectiveness of drive, gearing mechanism and tank chassis mechanisms, respectively.

Using following parameters m = 5 kg; r_H = 0,029 m; α = 30°; P = 0,01769 m^2; v = 20 ms^{-1}; η_{PA} = 1;η_{PR} = 0,96; η_{PM} = 0,9, can be determined required torque of actuator:

$$M_{Real} = \frac{M}{\eta_T} \rightarrow M_{Real} > 6{,}82 kg.cm. \tag{7}$$

2.2.2. Lateral Motion of Robot on Inclined Plane

The inner forces acting on moving robot during lateral motion are the same like for the case of linear motion. Therefor in this section will be dealt only with external forces.

For lateral (curvilinear) motion is characteristic, that in every time there is an axis of rotation with midst O.

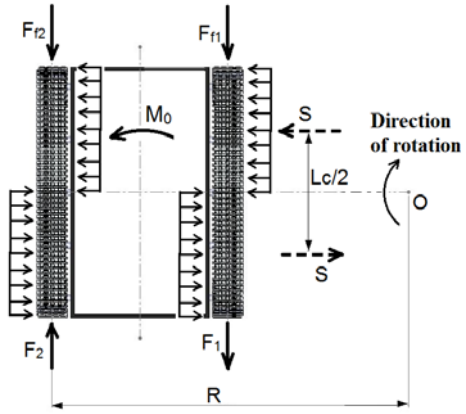

Figure 5. Forces acting on moving robot during rotation

Considering Figure 5, M_0 is moment acting to opposite of lateral motion. It can be described as

$$M_0 = \mu F_T L_C \frac{1}{4} \tag{8}$$

where μ is coefficient of resistance during lateral motion. It can be expressed as

$$\mu = \frac{\mu_{\max}}{\beta + (1-\beta)\frac{R}{\beta}} = \frac{1}{0{,}8 + (1-0{,}8)1} = 1 \tag{9}$$

where μ_{max} coefficient which depends on surface (in this case it is grass surface). Next, β is coefficient which is in the range of values 0,8 – 0,87. Coefficient S is total force, whichacting on tank chassis.

$$S = \mu p L_C \frac{1}{2} \tag{10}$$

where p is normal force acting on unit surface:

$$p = \frac{F_T}{2L_C} \tag{11}$$

Forces F_{f1}, F_{f2} are rolling-resistance forces and F_1 and F_2 are propulsive forces acting on tank chassis during lateral motion. Considering above mentioned equations and angle of inclined plane α=30°, the final required torque of actuator is expressed as

$$M_{lReal} = \frac{M_l}{\eta_T} \rightarrow M_{lReal} > 9{,}84 kg.cm \tag{12}$$

Based on above mechanical analysis the propulsive actuator for tank chassis was chosen, servomechanism

Monza SSA120M. Dimensions of servomechanism are 40,7 x 42,9 x 20 mm, weight is 55 g and torque is 12 kg.cm.

Figure 6. Chosen servomechanism for generating of robot propulsive force

2.3. Design of Driving Axle

Motion of tank chassis robot is ensured by driving axle. In this case, driving axle consists of driving shaft, couple of bearings, bearing houses and clutch. Particular mechanical components are designed in SolidWorks. Using SolidWorks were also done FEM analysis.

2.3.1. Driving Shaft

Design of driving shaft shape is based on the shape and dimensions of driving wheel, see Figure 7. The shaft was designed so, that clutch can be attached from the other side, opposite to wheel.

Figure 7. Driving wheel

Shape and dimensions of driving shaft are shown in the Figure 8.

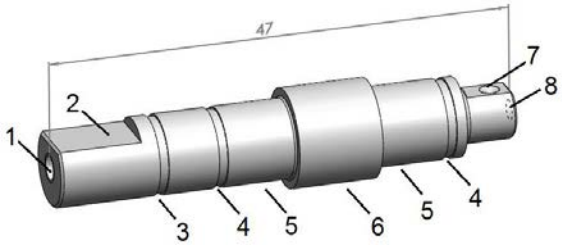

Figure 8. Driving shaft

where particular numbers represents following: 1 –hole with inner thread for screw M3 x 10 EN ISO 4762, which ensures axial position towards driving wheel; 2 – plane, which ensures transmission of torque to driving wheel; 3, 4 – recess for snap-ring; 5 – cylinder for bearing seating; 6 – cylinder for ensuring of axial position of bearing; 7 – hole for screw M2 x 10 EN ISO 8676, which ensures axial position of clutch towards shaft.

The material of shaft is steel EN 10027-1. The result of analysis is shown in the Figure 9. Load force for FEM analysis is only estimated and slightly oversized. The real load force has not been already determined in this phase, because all components are not designed yet.

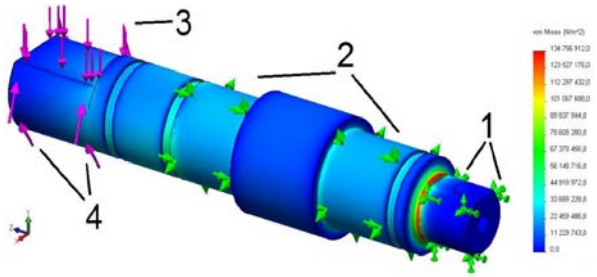

Figure 9. Strength analysis of driving shaft

For FEM analysis was used static state, because of too low velocity of robot during the applications. The maximal strength is σ=134,75MPa, what is admissible value.

2.3.2. Bearing House

The bearing house is used for fixing bearing position. Main parameter for designing of bearing house is outer diameter of bearing. Also, considering other aspects like other subcomponents of driving axle, the final shape of bearing house is shown in the Figure 10.

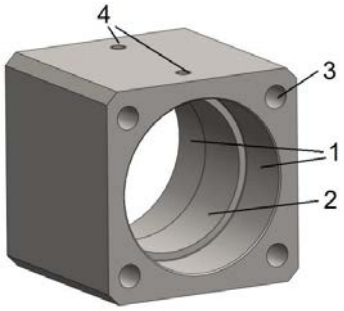

Figure 10. Bearing house of driving axle

where 1 – plane for bearing seating; 2 – cylinder with diameter 20 mm for ensuring of axial position of bearing; 3 –holes for screws M3 x 35 EN ISO 4762 for ensuring position towards bodywork; 4 –holes for screws with diameter M3 x 4 EN ISO 4762, which ensures axial position of bearing. As bearing house material was considered polyamide 6 or aluminium alloy AlCu4Mg. In both cases the price of the bearing house would increase, there for the material of bearing house is steel. Using steel, the weight of bearing house doesn´t rapidly increase. Subsequently, the strength analysis of bearing house was done, see Figure 11.

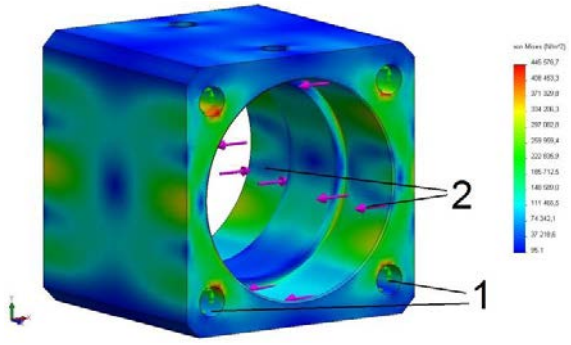

Figure 11. Strength analysis of bearing house

where 1 – constraint (place of screws); 2 – forces of bearings acting on the bearing house. The maximal determined strength is σ=0,446 MPa, what is admissible value.

2.3.3. Design of Clutch

The clutch is used for transmission of motor torque from outer shaft of servomechanism to driving axle. The clutch is designed so, that it can be easily connected with carrier of servomechanism, see Figure 12.

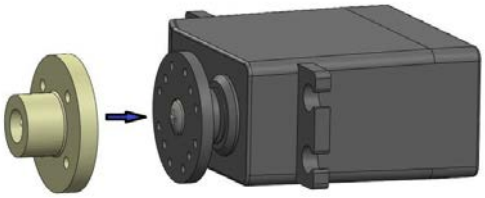

Figure 12. Clutch for servomechanism

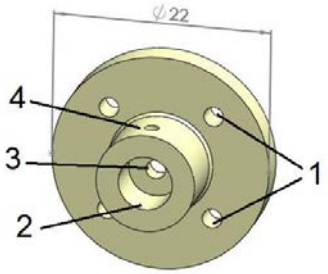

Figure 13. Clutch

where 1 –holes for screws M2 x 8 EN ISO 4014, which ensure transmission of torque from carrier to clutch; 2 – cylinder for seating of driving axle; 3 –hole for screw M2 x 10 EN ISO 8676, which ensures axial position towards shaft; 4 –hole for screw ST2,2 x 5 EN ISO 7049, which is insured. The material of clutch is polyamide 6. Strength analysis of clutch is shownin the Figure 14.

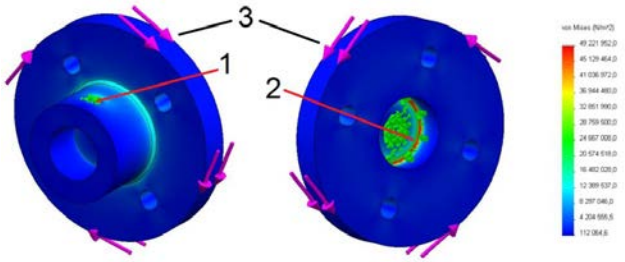

Figure 14. Strength analysis of clutch

where 1 – constraint in place of screw; 2 – constraint representing friction between screw head and contact surface on clutch; 3 – torque, which is transmissed from carrier to clutch. From the strength analysis the maximal strength is σ=49,2MPa.

2.3.4. Final State of Driving Axle

After designing of particular components of driving axle, the final 3D model is shown in the Figure 15 - Figure 16.

2.4. Design of Powered Axle

The powered axle has to realize mechanic support for tank chassis as well as stretching it by force F_S. The first step is to design a suitable powered wheel, which would have the same diameter as driving wheel. In this case, for the powered wheel was used the same wheel as for driving wheel.

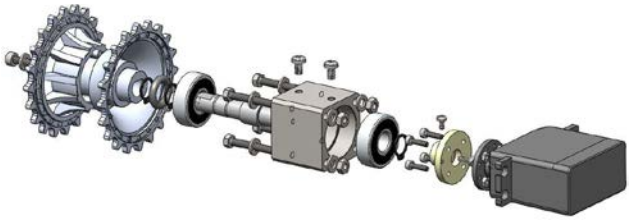

Figure 15. Final version of driving axle - decomposed

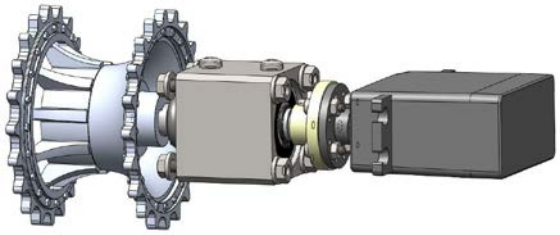

Figure 16. Final version of driving axle - composed

Next step is to design a powered shaft.For simplification, powered shaft will be almost identical with driving shaft, see Figure 17.

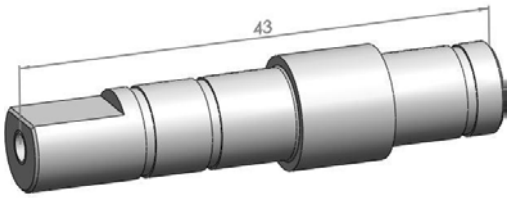

Figure 17. Powered shaft

Considering, that the material of driving and powered shaft is the same, while powered axle is not affected by torque of servomechanism, the strength analysis doesn´t have to be performed.

The stretching of tank chassis works on principle of shifting of powered axle in the direction of the force F_S. This shifting is ensured by turning of screw, see Figure 18.

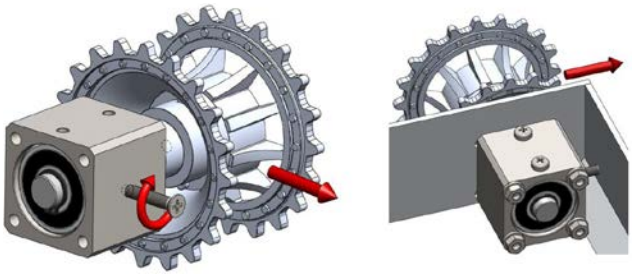

Figure 18. Shifting of powered axle in the direction of force F_S

By turning of screw can be achieved the movement of powered axle as well as stretching of tank chassis. Bearing house and stretching screw have to be properly bounded to bodywork of robot. The head of stretching screw leans on wall of bodywork, while mutual position of bearing house and side wall is ensured by screws M3 x 35 EN ISO 4762. During process of stretching they are released and after achievement of suitable stretching they are screwed.

The final state of powered axle is shown in the Figure 19.

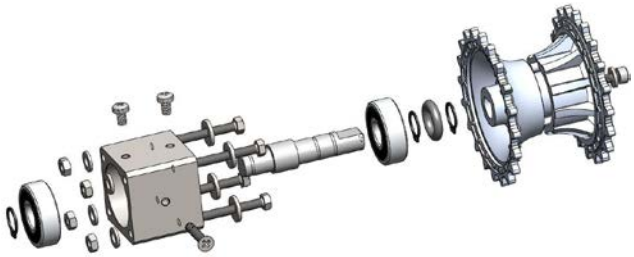

Figure 19. Final version of powered axle - decomposed

2.5. Design of Idle Wheels System

The idle wheels system provides holding-down of bottom part of tank chassis to the surface. This system consists of three main parts, namely idle wheels, shafts and houses for shafts seating, see Figure 20.

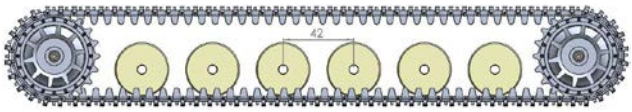

Figure 20. System of idle wheels

For material of wheels was chosen polyamide 6. Its big advantage is low specific weight and low friction coefficient. Final model of mentioned system is shown in the Figure 21.

Figure 21. System of idle wheels - decomposed

Considering all above mentioned components in driving and powered axle, the final mechanical model of tank chassis robot can be introduced in the Figure 22.

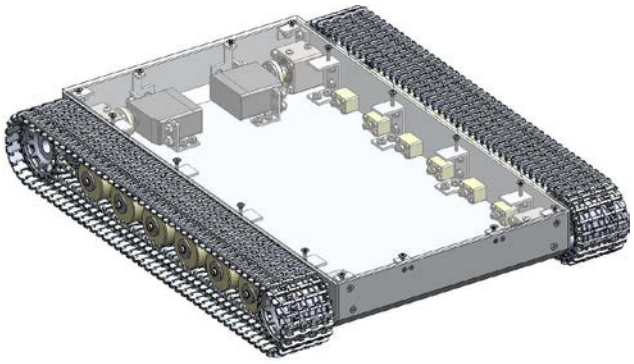

Figure 22. Mechanical model of tank chassis inspection robot

From the Figure 22 can be seen, that there is o a lot of free space inside of robot. Nevertheless, these dimensions of robot will used for final model. Using a significantly smaller shape of robot, the stability would be not sufficient andduring application on rough terrain would robot overturns.

3. Design of Electrical Parts of Robot

The inspection mobile robot has to dispose with several properties, by which it can perform, in this case, detection of undercarriage of car. At first, the inspection mobile robot should provide video signal from the inspection. Next, it should be able to record acoustic signal from inspected area. During all inspection process should be user remote from inspected area, because of potential explosions presence. Other requirements for inspection robot depend on specific application, which will robot performs.

Based on all required possibilities of inspection should be designed electromechanical components.

3.1. Camera System

Robot contains two cameras, one at rear and one in the front of robot. Rear camera is placed statically. For front camera the position mechanism is designed, see Figure 23.

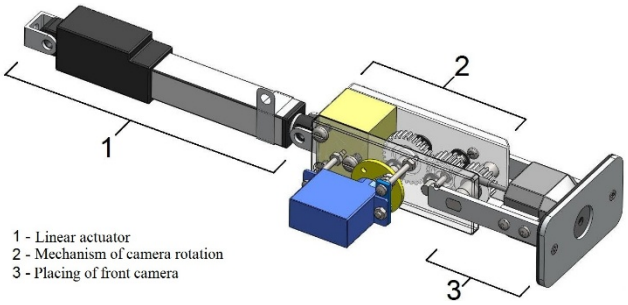

Figure 23. Position mechanism of front camera

For linear motion was used linear servomechanism Firgelli L12 with stroke 50 mm and for revolute motion was used servomechanism Hitec HS-50. These servomechanisms create in combination with gearbox positioning mechanisms of camera. Front camera is ZT-811T from the company Zhong Wang Electronics. Frequency range of the camera is 2,4 GHz.

In the following figure, the positioning system of front camera is shown.

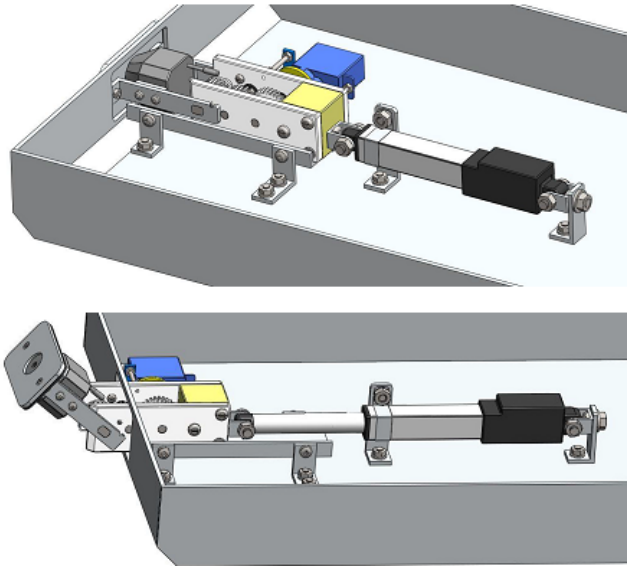

Figure 24. Positioning mechanism of front camera

3.2. Lighting of Undercarriage

For motion of robot in the night, it is necessary to equip the robot with light emitters. For this purpose the system

of LEDs was designed. Luminance of these LEDs is up to 20 cd. In order to saving of electric energy, the automatic system of lighting is designed. The principle of the system is based on using of light-dependent resistor, which changes its electric resistance depending upon light intensity.

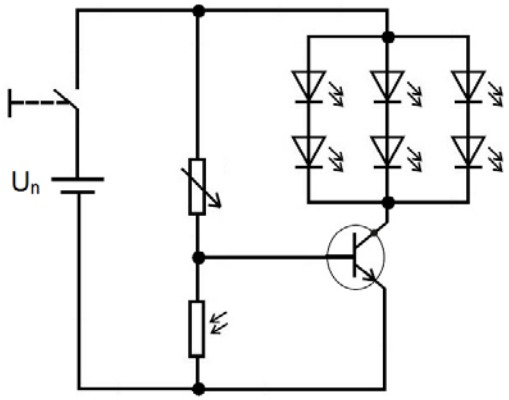

Figure 25. Electric circuit of lighting system

Electric resistance of light-dependent resistor is 10kΩ and resistance of rotary trimming resistor is 100 – 10 kΩ. Used transistor is used BC337-40BK with maximum current of collector 1 A.

3.3. Determination of Electric Power Supply

Determination of electric power consumption is important point in order to suitable accumulator can be chosen. There is an assumption, that robot should work sat least one hour without charging of accumulator. Approximate value of capacity of accumulator can be determined according to following equation:

$$C_T = I_T t \tag{13}$$

where t is required holding time of accumulator and I_T is total electric current consumption, which can be described as:

$$I_T = I_A + I_{OLED} + I_{ILED} + I_{CAM} \tag{14}$$

where I_A is current, required by actuators of robot (2x800 mAh), I_{OLED} is current of all illumining LEDs (8x25 mAh), I_{ILED} is current of indicator LEDs (3x20 mAh) and I_{CAM} is current of cameras (2x100 mAh). Assuming all mentioned consumers of electric current, total required capacity of accumulator is 1960 mAh. For the calculation was assumed the extreme case, when all consumers of current are used non-stop during one hour. Calculation didn´t assume current of rotation camera system, because these motors are not used non-stop during application of robot. Based on above analysis, there was chosen accumulator NiMH with capacity 3000 mAh.

Final state of electromechanical components are shown in the Figure 26.

4. Conclusion

The paper is focused on designing of mechanical and electronic parts of mobile inspection robot. The main aim of the robot is inspection of car under carriage, due to possible explosives presence. Robot is able to transmit video signal to safety distance to operator, which can control the robot by RC set. The robot can moves on rough terrain stably and effective because of tank chassis. The final parameters of the robot are:
Weight: 4432,91 g
Dimensions: 305 x 58 x 370 mm
Velocity: 16 cm/s.

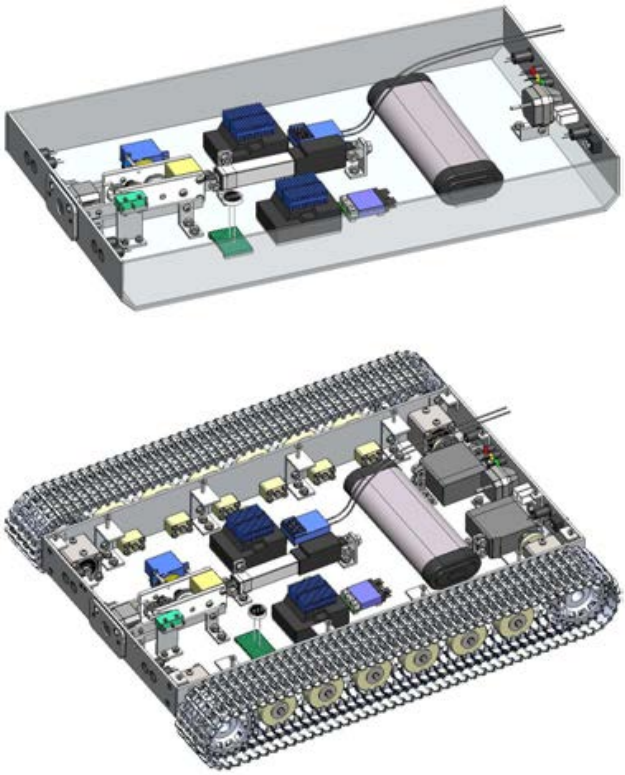

Figure 26. Electromechanical components of the robot

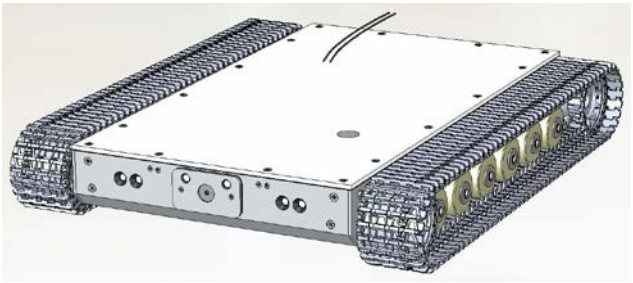

Figure 27. Final 3D model of the robot

Figure 28. Final version of designed inspection mobile robot

Acknowledgement

The authors would like to thank to Slovak Grant Agency – project VEGA 1/1205/12 "Numerical modelling of mechatronic systems". This contribution is also result of the project APVV-0091-11 “Using of methods of experimental and numerical modeling for increasing of competitiveness and innovation of mechanical and mechatronical systems” and KEGA project no. 048TUKE-4/2014 “Increasing of knowledge base of students in area of application of embedded systems in mechatronic systems”.

References

[1] Smrček, J; Kárník, L.:Robotika - Servisnéroboty - navrhovanie, konštrukcia, riešenia, Košice, 2008.

[2] Babinec, A., Vitko, A., Duchoň, F., Dekan, M.: Navigation of Robot Using VFH+ Algorithm, Journal of Mechanics Engineering and Automation 3 (2013), pp. 303-310.

[3] Božek, P.: Control of a Robotic Arm on the Principle of Separate Decision of an Inertial Navigation System, Applied Mechanics and Materials (2014), pp. 60-66.

[4] Giergiel, M., Buratowski, T., Malka, P.: The Mathematical Description of the Robotfor the Tank Inspection, Mechanics and Mechanical Engineering (2011), Vol. 15, No. 4, pp. 53-60.